Heliyon 11 (2025) e42197

Contents lists available at ScienceDirect

Heliyon

journal homepage: www.cell.com/heliyon

Research article

Lipids as key biomarkers in unravelling the pathophysiology of obesity-related metabolic dysregulation

Anis Adibah Osman [a], Siok-Fong Chin [a,*], Lay-Kek Teh [b,c], Noraidatulakma Abdullah [a], Nor Azian Abdul Murad [a], Rahman Jamal [a,**]

[a] UKM Medical Molecular Biology Institute (UMBI), Universiti Kebangsaan Malaysia, Jalan Yaacob Latif, Bandar Tun Razak, Cheras, Wilayah Persekutuan, 56000, Kuala Lumpur, Malaysia

[b] Integrative Pharmacogenomics Institute (iPROMISE), Universiti Teknologi MARA, Puncak Alam Campus, 42300, Bandar Puncak Alam, Selangor, Malaysia

[c] Faculty of Pharmacy, Universiti Teknologi MARA, Puncak Alam Campus, 42300, Bandar Puncak Alam, Selangor, Malaysia

ARTICLE INFO

Keywords:
Obesity
Untargeted metabolomics
Pathogenesis
Metabolic signatures
Prediction model

ABSTRACT

Background and objective: Obesity is intricately linked with metabolic disturbances. The comprehensive exploration of metabolomes is important in unravelling the complexities of obesity development. This study was aimed to discern unique metabolite signatures in obese and lean individuals using liquid chromatography-mass spectrometry quadruple time-of-flight (LC-MS/Q-TOF), with the goal of elucidating their roles in obesity.

Methods: A total of 160 serum samples (Discovery, n = 60 and Validation, n = 100) of obese and lean individuals with stable Body Mass Index (BMI) values were retrieved from The Malaysian Cohort biobank. Metabolic profiles were obtained using LC-MS/Q-TOF in dual-polarity mode. Metabolites were identified using a molecular feature and chemical formula algorithm, followed by a differential analysis using MetaboAnalyst 5.0. Validation of potential metabolites was conducted by assessing their presence through collision-induced dissociation (CID) using a targeted tandem MS approach.

Results: A total of 85 significantly differentially expressed metabolites (p-value <0.05; $-1.5 < FC > 1.5$) were identified between the lean and the obese individuals, with the lipid class being the most prominent. A stepwise logistic regression revealed three metabolites associated with increased risk of obesity (14-methylheptadecanoic acid, 4′-apo-beta,psi-caroten-4'al and 6E,9E-octadecadienoic acid), and three with lower risk of obesity (19:0(11Me), 7,8-Dihydro-3b,6a-dihydroxy-alpha-ionol 9-[apiosyl-(1->6)-glucoside] and 4Z-Decenyl acetate). The model exhibited outstanding performance with an AUC value of 0.95. The predictive model underwent evaluation

Abbreviations: AAA, Aromatic amino acid; ACN, Acetonitrile; AUC, Area under curve; BCAA, Branched-chain amino acid; BCFA, Branched-chain fatty acid; BIA, Bioelectrical impedance analysis; BMI, Body mass index; Cl, Confidence interval; CID, Collision-induced dissociation; ddH_2O, Double distilled water; DXA, Dual X-Ray absorptiometry; EIC, Extracted ion chromatogram; FC, Fold change; HDL, High density lipoprotein; LC-MS/Q-TOF, Liquid chromatography-mass spectrometry quadruple time-of-flight; MPP, Mass profiler professional; OR, Odds ratio; PLS-DA, Partial least square – discriminative analysis; QC, Quality control; ROC, Receiver operating characteristic; RSD, Relative standard deviation; SVM, Support vector machine.

* Corresponding author. UKM Medical Molecular Biology Institute (UMBI), Universiti Kebangsaan Malaysia (UKM), Jalan Yaacob Latif, Bandar Tun Razak, Cheras, 56000, Kuala Lumpur, Malaysia.

** Corresponding author. UKM Medical Molecular Biology Institute (UMBI), Universiti Kebangsaan Malaysia (UKM), Jalan Yaacob Latif, Bandar Tun Razak, Cheras, 56000, Kuala Lumpur, Malaysia.

E-mail addresses: chinsiokfong@hctm.ukm.edu.my (S.-F. Chin), rahmanj@hctm.ukm.edu.my (R. Jamal).

https://doi.org/10.1016/j.heliyon.2025.e42197
Received 22 July 2024; Received in revised form 6 December 2024; Accepted 21 January 2025
Available online 23 January 2025

across four machine learning algorithms consistently demonstrated the highest predictive accuracy of 0.821, aligning with the findings from the classical logistic regression statistical model. Notably, the presence of 4′-apo-beta,psi-caroten-4′-al showed a statistically significant difference between the lean and obese individuals among the metabolites included in the model.
Conclusions: Our findings highlight the significance of lipids in obesity-related metabolic alterations, providing insights into the pathophysiological mechanisms contributing to obesity. This underscores their potential as biomarkers for metabolic dysregulation associated with obesity.

1. Introduction

Obesity presents a multifaceted challenge, marked by the excessive accumulation of body fat, and a subsequent risk to health [1]. Global obesity rates have surged nearly threefold since 1975, impacting over 650 million adults worldwide. In Malaysia, abdominal obesity currently affects at least one in two individuals [2]. These alarming statistics underscore the urgent need for more effective strategies to reduce obesity cases.

The aetiology of this condition is complex, encompassing genetic, epigenetic, and environmental factors such as sedentary lifestyles [3–5]. However, relying solely on genes and the related proteins cannot completely elucidate the pathogenesis of obesity, as genome abnormalities and non-functional proteins may obscure the clinical manifestations.

Metabolomics, the assessment of metabolites in a biological sample, offers a glimpse into the outcome of cellular pathways. Metabolites, defined as small molecules with a molecular weight less than 1500 Da, actively engage in dynamic roles within biological processes and signalling pathways contributing to the intricate regulation of metabolism. They have the capacity to capture molecular changes across the genome, transcriptome, and proteome [6]. In the context of obesity, alterations in metabolite levels serve as metabolic indicators that may elucidate the disease pathogenesis and their effects on the body [7–9].

The metabolism of obese individuals is found to exhibit significant differences compared to their lean counterparts [10–13]. Elevated levels of protein-based metabolites, including branched-chain amino acids (BCAA) and aromatic amino acids (AAA) are associated with obesity and insulin resistance, ultimately leading to the development of type II diabetes mellitus [14]. Moreover, various lipid-based metabolites, such as fatty acids, glycerophospholipid, sphingomyelin and acylcarnitine are claimed to be related to insulin regulation and inflammation [15]. However, studies have struggled to replicate identical metabolic profiles across obesity

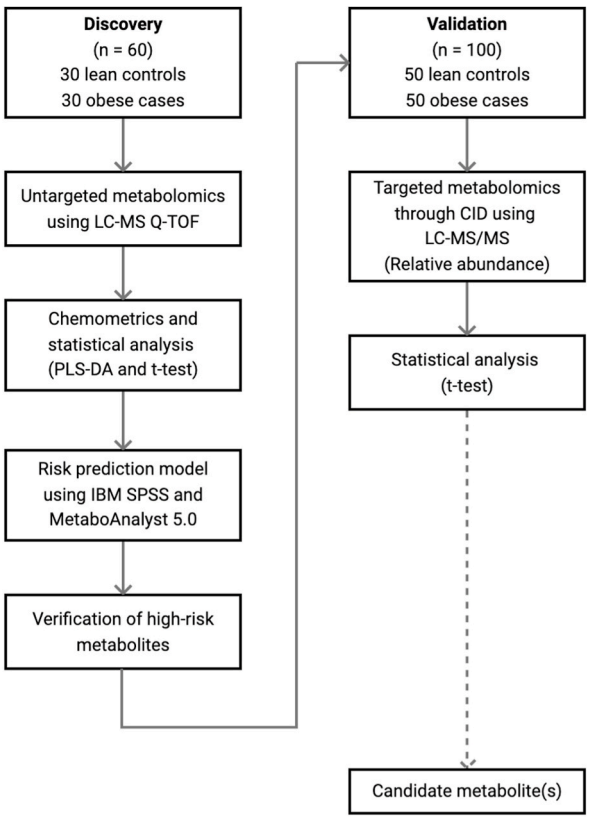

Fig. 1. Flowchart of the study.

cases. While genetics play a role in susceptibility to obesity, they account for only a small portion of its overall prevalence. The genetic variants identified to date explain only 5–10 % of the estimated heritability of the obesity phenotype [16]. Hence, understanding the complex interaction between genetic predispositions and environmental factors is essential for addressing the obesity epidemic.

This nested case-control study aims to illuminate the underlying mechanisms of obesity by characterising the metabolic signatures in both obese and lean individuals via metabolomics techniques. To our knowledge, this represents the first comprehensive metabolomics investigation focused on obesity within the Malaysians population, holding immense potential for unravelling metabolite-obesity relationships across our diverse ethnic and cultural landscape. Furthermore, this study represents a significant stride forward in realising the goals of precision medicine and precision nutrition.

2. Materials and methods

2.1. Sample selection

Participants were recruited from The Malaysian Cohort project who came for follow-up between September 2020 to December 2022 and residing in Kuala Lumpur and Selangor. The details of this project have been describe elsewhere [17]. This study adopted an extreme-value design strategy for sample selection; including cases involving individuals classified as obese, with a stable BMI of $\geq$30 kg/m^2, while control group participants were selected based on their consistent normal BMI within the range of 18.5–22.9 kg/m^2 from baseline to their most recent follow-up appointment. The rationale behind this approach was to encompass the broadest spectrum of BMI values while preventing any overlap between the control and case participants. Moreover, individuals with a history of cancer, thyroid or cardiovascular diseases, those taking medications for hypertension or lipid-lowering, as well as pregnant women at the beginning of the study, were excluded from participation in both case and control groups. The study protocol adhered to the principles outlined in the Helsinki Declaration and received approval from the Research Ethics Committee at Universiti Kebangsaan Malaysia (JEP-2021-344). The schematic representation of the study is illustrated in Fig. 1.

In the discovery phase of the study, we included 60 samples, ensuring a balanced representation of genders and ethnicities among both cases and controls. Subsequently, during the validation phase, we expanded the sample size to 100 based on calculations derived from the discovery phase. This expansion aimed to achieve a study power of 80 % while maintaining a type I error rate of $\alpha = 0.05$.

2.2. Sample preparation

Serum samples (50 μL) were mixed with 50 μL double distilled water (ddH_2O) adjusted to pH 10 and 400 μL of methanol. The mixture was vigorously vortexed at maximum speed for 30 s to ensure thorough mixing, followed by 10-min incubation on ice. Subsequently, centrifugation was performed at 19,000$\times g$ at 4 °C for 15 min (Eppendorf 5804R) and the supernatant was dried using a vacuum concentrator (Eppendorf 5301) for 1–2 h. The dried samples obtained were reconstituted by adding 30 μL of a solution containing 50 % methanol with 0.1 % formic acid. Following that, the mixture was then subjected to another round of vortexing and centrifugation. The resulting supernatant was then carefully transferred into an insert of the autosampler vial and queued for injection into the LC/MS system.

Similarly, the quality control (QC) sample, comprising an equal volume of all samples, also underwent the same process as the individual samples.

2.3. Untargeted metabolomics via LC/MS Q-TOF

Two modes were employed in the sample analysis: positive and negative ionization modes, each requiring a distinct mobile phase. In the positive mode, the mobile phase consisted of (A) double distilled water (ddH_2O) with the addition of 0.1 % formic acid and (B) acetonitrile (ACN) with 0.1 % formic acid. Conversely, in the negative mode, the mobile phase comprised (A) ddH_2O with the addition of 0.1 % ammonium formate and (B) ACN. The flow rate was set at 0.25 ml/min and 2 μL sample was injected into Agilent 6520 liquid chromatography-mass spectrometry quadruple time-of-flight (LC/MS Q-TOF) system. The reverse-phase liquid chromatography column used was Zorbax Eclipse Plus C18 600 Bar (2.1 $\times$ 100 mm, 1.8 μm).

In the positive mode, the mobile phase B was programmed to establish a linear gradient from 5 % to 95 % over 18 min, while in the negative mode, the gradient ranged from 50 % to 95 % over 15 min. The total running time was 23 min for the positive mode and 20 min for the negative mode, with the column temperature being consistently maintained at 40 °C throughout the analysis. Two internal reference masses were injected for each mode: 121.0509 and 922.0098 for the positive mode, and 112.9856 and 1033.9881 for the negative mode, serving as mass correction standards. Parameters for the electrospray ionization source included a capillary voltage of 4000 V, a skimmer voltage of 65 V, and a fragmentor voltage of 175 V. Additionally, the nebuliser pressure was adjusted to a pressure of 30 psi, and the nitrogen drying gas was maintained at a flow rate of 10 L/min, with a temperature of 325 °C.

The sample underwent analysis in four replicates, and quality control (QC) samples were injected at the beginning, middle, and end of the run to evaluate system performance and assay reproducibility. The precision and accuracy of each batch run were reviewed using the relative standard deviation (RSD), calculated by dividing the mean by the standard deviation of the selected metabolites. A predetermined threshold of 25 % was established as the acceptable RSD value for both within-day and between-day runs [18].

2.4. Data processing

Agilent Mass Hunter Workstation Software Qualitative Analysis Software Version B.05.00 was employed to perform initial processing of raw data. Metabolites were extracted using the molecular features algorithm within the 100–1000 *m/z* range for a duration of 0.00–18.00 min in positive mode and 0.00–15.00 min in negative mode. In positive mode, ion species were characterised with the addition of H^+, Na^+, K^+ and NH_4^+ as adducts. In contrast, in negative mode, the adducts utilized were H^-, Cl^-, Br^-, $HCOO^-$, CH_3COO^- and CF_3COO^-. A maximum charge limit of two was assigned to the metabolites, and data format conversion (.d to compound exchange file, cef) was performed using Agilent DA Reprocessor software. Subsequently, the data were transferred to Agilent Mass Profiler Professional (MPP) Version 12.1 for further analysis.

The detected metabolites were aligned with a retention time tolerance of 0.1 % + 0.15 min and a mass window of ±5.0 ppm +2.0 mDa. Filtering based on flags and frequency was implemented at a 50 % threshold to ensure that at least 50 % of the metabolites were consistently present in all technical replicates of the sample set. The annotation of metabolites was conducted by utilising the IDBrowser feature integrated with the Metlin database. Subsequently, the names of the metabolites were searched in various databases (PubChem, HMDB, ChEBI, and LipidMAPS), and details such as molecular weight and chemical formula were utilized to verify the

Table 1
Participants characteristics for both discovery (n = 60) and validation phases (n = 100).

Category	Discovery			Validation		
	Controls (n = 30)	Cases (n = 30)	*p*-value	Controls (n = 50)	Cases (n = 50)	*p*-value
Age, years (median (min-max))	56 (42–72)	51 (44–65)	0.066	58 (41–76)	54 (42–73)	**0.028***
Gender, n (%)						
Male	15 (50.0 %)	15 (50.0 %)	1.000	25 (50.0 %)	12 (24.0 %)	**0.007***
Female	15 (50.0 %)	15 (50.0 %)		25 (50.0 %)	38 (76.0 %)	
Race, n (%)						
Malay	10 (33.3 %)	10 (33.3 %)	1.000	16 (32.0 %)	20 (40.0 %)	0.687
Chinese	10 (33.3 %)	10 (33.3 %)		18 (36.0 %)	15 (30.0 %)	
Indian	10 (33.3 %)	10 (33.3 %)		16 (32.0 %)	15 (30.0 %)	
Occupation, n (%)						
Working	20 (66.7 %)	22 (73.3 %)	0.573	35 (70.0 %)	31 (62.0 %)	0.398
Not working	10 (33.3 %)	8 (26.7 %)		15 (30.0 %)	19 (38.0 %)	
Alcohol status, n (%)						
Yes	0 (0.0 %)	2 (6.7 %)	0.492	2 (4.0 %)	1 (2.0 %)	1.000
No/Former drinker	30 (100.0 %)	28 (93.3 %)		48 (96.0 %)	49 (98.0 %)	
Smoking, n (%)						
Yes	3 (10.0 %)	5 (16.7 %)	0.706	6 (12.0 %)	5 (10.0 %)	0.749
No/Ever smoked	27 (90.0 %)	25 (83.3 %)		44 (88.0 %)	45 (90.0 %)	
Anthropometry, mean (SD) or median (IQR)						
Height (cm)	160.88 (7.09)	161.43 (8.51)	0.787	160.74 (8.76)	159.71 (7.08)	0.443
Weight (kg)	52.17 (5.45)	96.76 (8.45)	**<0.001***	54.94 (6.71)	86.94 (9.87)	**<0.001***
BMI (kg/m^2)	20.18 (19.24–20.86)	35.65 (33.61–42.47)	**<0.001***	21.11 (20.53–22.19)	33.20 (31.43–35.76)	**<0.001***
Waist circumference (cm)	71.55 (6.14)	105.59 (8.86)	**<0.001***	75.18 (6.48)	98.77 (7.62)	**<0.001***
Hip circumference (cm)	89.32 (3.71)	120.13 (10.09)	**<0.001***	92.00 (89.00–94.00)	116.00 (109.50–118.50)	**<0.001***
Waist-to-hip ratio	0.80 (0.06)	0.88 (0.09)	**<0.001***	0.82 (0.07)	0.86 (0.06)	**0.013***
Clinical, mean (SD) or median (IQR)						
Systolic blood pressure (mmHg)	121.69 (16.58)	134.04 (21.66)	**0.016***	127.59 (16.47)	130.15 (15.55)	0.426
Diastolic blood pressure (mmHg)	69.06 (8.51)	81.72 (11.81)	**<0.001***	72.75 (9.63)	80.08 (9.18)	**<0.001***
Total cholesterol (mmol/L)	5.53 (0.98)	5.19 (0.80)	0.149	5.66 (5.07–6.26)	4.97 (4.52–6.00)	**0.023***
High-density lipoprotein (mmol/L)	1.66 (0.47)[a]	1.18 (0.26)	**<0.001***	1.73 (0.39)	1.35 (0.24)	**<0.001***
Low-density lipoprotein (mmol/L)	3.36 (0.93)	3.29 (0.65)	0.739	3.53 (2.76–3.88)	3.24 (2.56–3.80)	0.285
Triglyceride (mmol/L)	1.01 (0.76–1.38)	1.36 (1.02–2.00)	**0.008***	0.95 (0.77–1.25)	1.26 (1.00–1.70)	**<0.001***
Glucose (mmol/L)	5.15 (4.90–5.49)	5.47 (5.23–5.85)	**0.019***	5.28 (0.46)	5.65 (0.59)	**0.001***
HbA1c (%)	5.50 (5.15–5.73)	5.70 (5.35–6.00)	0.144	5.50 (5.20–5.70)	5.60 (5.40–5.90)	0.103
Insulin (μIU/mL)	4.44 (2.97–6.95)	15.06 (10.32–24.22)	**<0.001***	5.40 (3.52–7.80)	13.21 (10.49–19.94)	**<0.001***
HOMA-IR	1.01 (0.68–1.66)	3.87 (2.42–6.32)	**<0.001***	1.19 (0.75–1.94)	3.42 (2.49–5.44)	**<0.001***
HOMA-β	60.54 (36.90–76.22)	146.19 (110.52–198.85)	**<0.001***	64.57 (43.03–84.27)	145.77 (104.00–191.95)	**<0.001***

• Data are presented as median (min-max) for age, n (%) for categorical data, mean (SD) for normally distributed anthropometric and clinical parameters and median (IQR) for continuous data with a non-normal distribution. *p*-values were calculated using Pearson's χ^2 for categorical data and independent *t*-test and Mann-Whitney test for numerical data. A *p*-value <0.05 indicates a statistically significant difference between the cases and controls group, denoted by an asterisk (*).

[a] One data point is missing.

annotations.

2.5. Statistical analysis

The demography data of participants were analysed using IBM® SPSS software version 23. Univariable analysis of the identified metabolites was conducted using the Agilent MPP application, employing a *t*-test, with statistical significance set at a *p*-value threshold of less than 0.05. Furthermore, significant metabolites were selected based on a fold change threshold of less than −1.5 or greater than 1.5. This accounts for the fact that metabolite levels can vary in both directions, increasing or decreasing, hence the use of the plus-minus designation. As for the 1.5-fold change value, it is a commonly used threshold by researchers to identify differential metabolite expression [19]. A fold change greater than 1.5 indicates that the metabolite is overexpressed by 50 % in the obese group compared to the normal group, while a fold change less than 1.5 suggests that the metabolite is under-expressed by 50 % in the obese group compared to the normal group. This is considered biologically meaningful, as the change in metabolite levels reflects a difference in their expression. Next, recursion analysis was performed on the shortlisted metabolites. This step involves repeating data processing using a chemical formula algorithm to confirm metabolite identities. Given the dynamic nature of metabolites, we aimed to include a broader range for building a prediction model. Therefore, the significant metabolites were primarily selected based on their *p*-value and fold change. The metabolites also underwent multiple comparisons, with Benjamini-Hochberg correction to control the false discovery rate (FDR). The results from both positive and negative modes were merged and then exported to MetaboAnalyst 5.0 (http://www.metaboanalyst.ca/) for chemometric analysis. The prediction model of obesity using metabolites and combination of both metabolites and clinical data were achieved using the multiple logistic regression analysis within the SPSS software. The forest plot was generated using Prism version 9.5.1 to visualise the prediction model.

2.6. Validation of potential metabolites

A new set of samples (n = 100) underwent a preparation process similar to the one previously described, with a minor adjustment. The sample volume was increased to 100 μl, and the injection volume into the instrument was also raised to 10 μl. This adjustment aimed to enhance the abundance of metabolites within the samples.

The targeted tandem MS was configured using the retention time and mass data of potential metabolites identified during the discovery phase. Metabolites selected from the prediction model were subjected to collision-induced dissociation (CID) at 20 V to generate product ion fragments from the parent ions. The relative abundance of each metabolite was compared between the case and control groups using the extracted ion chromatogram (EIC). To validate the presence of chosen metabolite, fragments were compared to the in-silico spectra predictions generated by competitive fragmentation modelling for metabolite identification (CFM-ID 4.0), with specific consideration for the spectra type, ion mode, and adduct type [20]. Three sets of spectra were overlapped at different energy levels (low - 10 V, middle – 20 V, and high – 40 V) to identify common fragments and their similarity and stability were assessed. The abundance of each metabolite was compared using a *t*-test, with a *p*-value of less than 0.05 considered statistically significant.

3. Results

3.1. Participants characteristics

Table 1 presents the characteristics of the participants. The majority of the participants were employed, non-alcohol drinkers, non-smokers and with ages that ranged from 41 to 72 years old. In the discovery phase, both the case (obese) and control (lean) groups showed no statistically significant differences across all demographic categories. However, significant differences in age and gender were observed between lean and obese in the validation data. During the discovery phase, all anthropometric parameters exhibited higher mean values in the obese group compared to the lean group. Among these parameters, only height did not show a statistically significant difference between the two groups. The validation data demonstrated a similar trend to the discovery data, although in this case, obese participants had a lower mean height compared to the leans.

In terms of clinical parameters, both the discovery and validation datasets exhibited significant higher mean or median values in cases compared to controls, with the exception of high-density lipoprotein (HDL), which displayed significantly lower mean values in cases compared to controls. Furthermore, diastolic blood pressure, HDL, triglyceride, glucose, insulin, HOMA-IR, and HOMA-β demonstrated significant differences between the cases and controls in both datasets. Regarding body composition, all parameters showed significantly higher mean values in cases compared to controls as detailed in Table S1. There were also statistically significant differences in body composition assessment between cases and controls in both the discovery and validation data, as measured by both InBody 770 BIA (bioelectrical impedance analysis) (Biospace, USA) and Discovery A DXA (Dual X-Ray Absorptiometry) (Hologic®, USA) instruments.

3.2. Metabolite identification

Untargeted metabolomics analysis via molecular feature search in Mass Profiler Professional (MPP) yielded more entities in negative mode (82,240) than in positive mode (67,182). Following filtering by flag and frequency, 556 and 674 metabolites were identified in positive and negative mode, respectively. After annotation using the Metlin database and the removal of duplicate entries across modes, a total of 438 metabolites were selected for subsequent statistical analysis. Among these, only 85 metabolites exhibited

statistically significant differences, defined by a p-value <0.05 and a fold change (FC) between -1.5 and 1.5. Recursive analysis based on chemical formula revealed a similar number of metabolites. This step aims to minimize the occurrence of false-positive metabolite identifications. Subsequently, the identified metabolites underwent cross-referencing with the PubChem, HMDB, ChEBI, and LipidMAPS databases to enhance the reliability of metabolite identification. A summary of the strategies employed for metabolite identification and statistical analysis is detailed in Fig. 2.

The Partial Least Squares Discriminant Analysis (PLS-DA) plot highlights the disparities in metabolite profiles between lean individuals (BMI range: 18.5–22.9 kg/m^2) and obese individuals (BMI $\geq$30 kg/m^2). In the plot, a noticeable clustering of controls (lean individual represented by blue circles) and cases (obese individuals in pink circles) is evident for the identified metabolites. Moreover, significant metabolites exhibit even clearer separation between the two groups, as illustrated in Fig. 3. These findings underscore the existence of a distinct metabolic profile associated with obesity.

Among the significantly expressed metabolites, lipids were the most commonly identified class in the studied groups. Furthermore, this class was consistently highly represented in both the upregulated (64.5 %) and downregulated (64.8 %) metabolites (Fig. 4(a)–(c)). The top upregulated metabolite identified was a lipid; 4′-apo-beta,psi-caroten-4′-al (FC = 37.11, adjusted p-value = 2.28×10^{-5}), while the leading downregulated metabolite was also classified as a lipid, known as unanisoflavan (FC = 18.41, adjusted p-value = 0.01). A full list of the identified metabolites with fold change and p-values are provided in Table S3. The Metabolite Set Enrichment Analysis (MSEA) (Fig. 4 (d)) revealed glycerophospholipid metabolism as the pathway most significantly altered in our dataset (p-value = 0.005).

3.3. Prediction of metabolites related to obesity

A stepwise multiple logistic regression model was constructed to predict the potential association of combination metabolite with obesity. Initially, all significant metabolites were included as independent variables using both forward and backward likelihood methods, and the selection of metabolites was based on those that remained significant within the model without any adjustment. Fig. 5 (a) illustrates a forest plot that highlights six significant metabolites: three associated with an increased risk of obesity (odds ratios (OR) greater than 1), and the other three with a lower risk of obesity (odds ratios less than 1). The metabolites associated with a higher risk of obesity include 14-methylheptadecanoic acid (OR = 12.669, 95 % CI = 1.808–88.750, p-value = 0.011), 4′-apo-beta,psi-caroten-4'al (OR = 1.282, 95 % CI = 1.054–1.559, p-value = 0.013) and 6E,9E-octadecadienoic acid (OR = 1.213, 95 % CI = 1.006–1.464, p-value = 0.043). Conversely, the metabolites associated with a lower risk of obesity include 19:0 (11Me) (OR = 0.811,

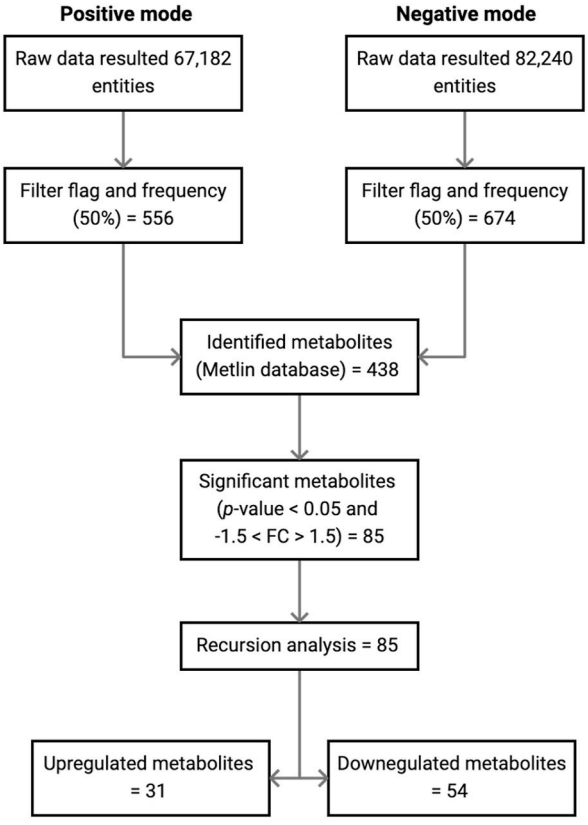

Fig. 2. Workflow for metabolite identification and statistical analysis.

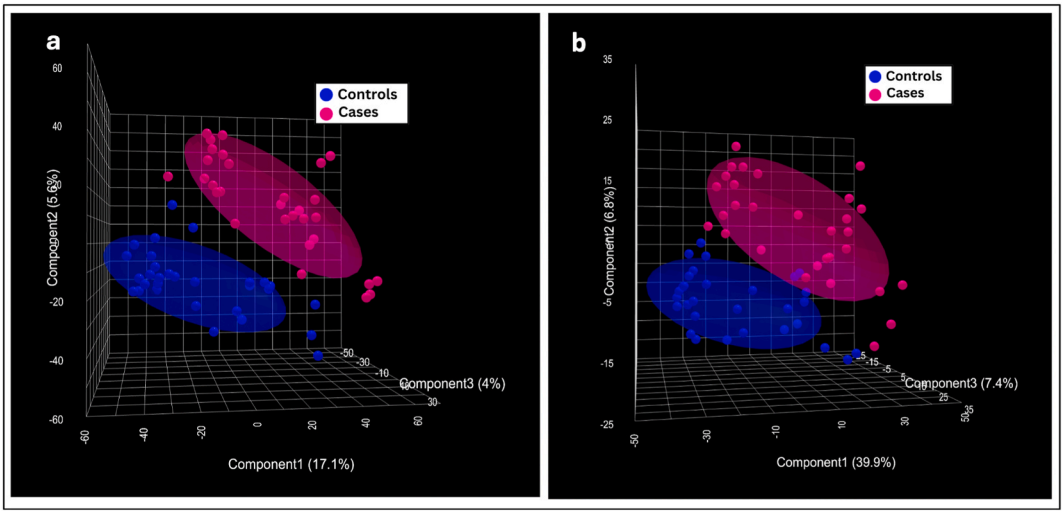

Fig. 3. PLS-DA plot illustrating metabolite profile differences between lean and obese individuals in (a) all identified metabolites, and (b) only significant metabolites, presented in 3D visualisation. Each data point represents an individual participant, with obese individuals depicted in pink circles, and lean individuals in blue circles. The distinct clustering of data points indicate significant differences in metabolite composition between the two groups, highlighting the potential metabolic dysregulation associated with obesity.

95 % CI = 0.670–0.982, *p*-value = 0.032), 7,8-Dihydro-3b,6a-dihydroxy-alpha-ionol 9-[apiosyl-(1->6)-glucoside] (OR = 0.756, 95 % CI = 0.596–0.958, *p*-value = 0.021) and 4Z-Decenyl acetate (OR = 0.656, 95 % CI = 0.494–0.872, *p*-value = 0.004). A Receiver Operating Characteristic (ROC) curve was generated based on these six selected metabolites to evaluate the model's discriminative ability between lean and obese individuals, revealing an exceptional Area Under the Curve (AUC) of 0.950. Incorporating participants' demographic characteristics into the model preserved the significance of each metabolite, resulted in a similar ROC curve, and maintained a consistent AUC value.

Our final model, which incorporated both metabolites and clinical parameters linked to obesity using multiple logistic regression was presented in a forest plot (Fig. 5 (b)). This model was built using significant clinical parameters alongside the metabolites model, and only the variables that remained significant were retained. Interestingly, our final predictive model revealed that 4′-apo-beta,psi-caroten-4'al (OR = 1.211, 95 % CI = 1.016–1.443, *p*-value = 0.033), 7,8-Dihydro-3b,6a-dihydroxy-alpha-ionol 9-[apiosyl-(1->6)-glucoside] (OR = 0.772, 95 % CI = 0.601–0.991, *p*-value = 0.043), along with two clinical variables, fasting blood glucose (OR = 3.569, 95 % CI = 1.212–10.509, *p*-value = 0.021) and HOMA-β (OR = 1.060, 95 % CI = 1.025–1.096, *p*-value = 0.001), were found statistically significant predictors of obesity in Malaysian population. This composite model effectively discriminated between lean and obese individuals, yielding a marginally improved AUC of 0.970, as illustrated in the ROC curve generated.

The identical model of these six metabolites was applied to various machine learning algorithms using 'ROC curve based model evaluation (Tester)' function within the web-based tools of MetaboAnalyst 5.0 (Table 2). Among the four algorithms tested, PLS-DA exhibited the lowest predictive accuracy at 0.735, while logistic regression achieved the highest predictive accuracy at 0.821. This outcome was consistent with our classical statistical model, exhibiting a robust ability to predict obesity.

Both the study power and effect size for each of the selected metabolites incorporated into the predictive model were computed (Table 3). The statistical power of five of the metabolites exceeded 0.8, indicating robust statistical strength. However, only 4Z-Decenyl acetate exhibited a study power of 0.63. According to Cohen's criteria, all six metabolites exhibited a medium effect size with $d > 0.5$, signifying that the differences in metabolite levels between groups had a moderate practical significance [21]. Based on these data, the sample size for validation was determined.

3.4. Performance of individual metabolites

The ROC curve (Fig. 6) was constructed to evaluate the performance of each selected metabolite included in the model. The metabolite that exhibited the highest performance was 14-methylheptadecanoic acid, with an AUC of 0.743 (95 % CI = 0.597–0.862), followed closely by 4′-apo-beta,psi-caroten-4′-al, which had an AUC of 0.721 (95 % CI = 0.594–0.833). All other metabolites achieved AUC values exceeding 0.6.

The presence of each metabolite was validated using LC-MS/MS, and the comparison of metabolite abundance was performed using extracted ion chromatogram (EIC). A log transformation was implemented to reduce data skewness. From Fig. 7, only 4′-apo-beta,psi-caroten-4′-al exhibited a statistically significant difference between controls and cases (*p*-value = 0.017).

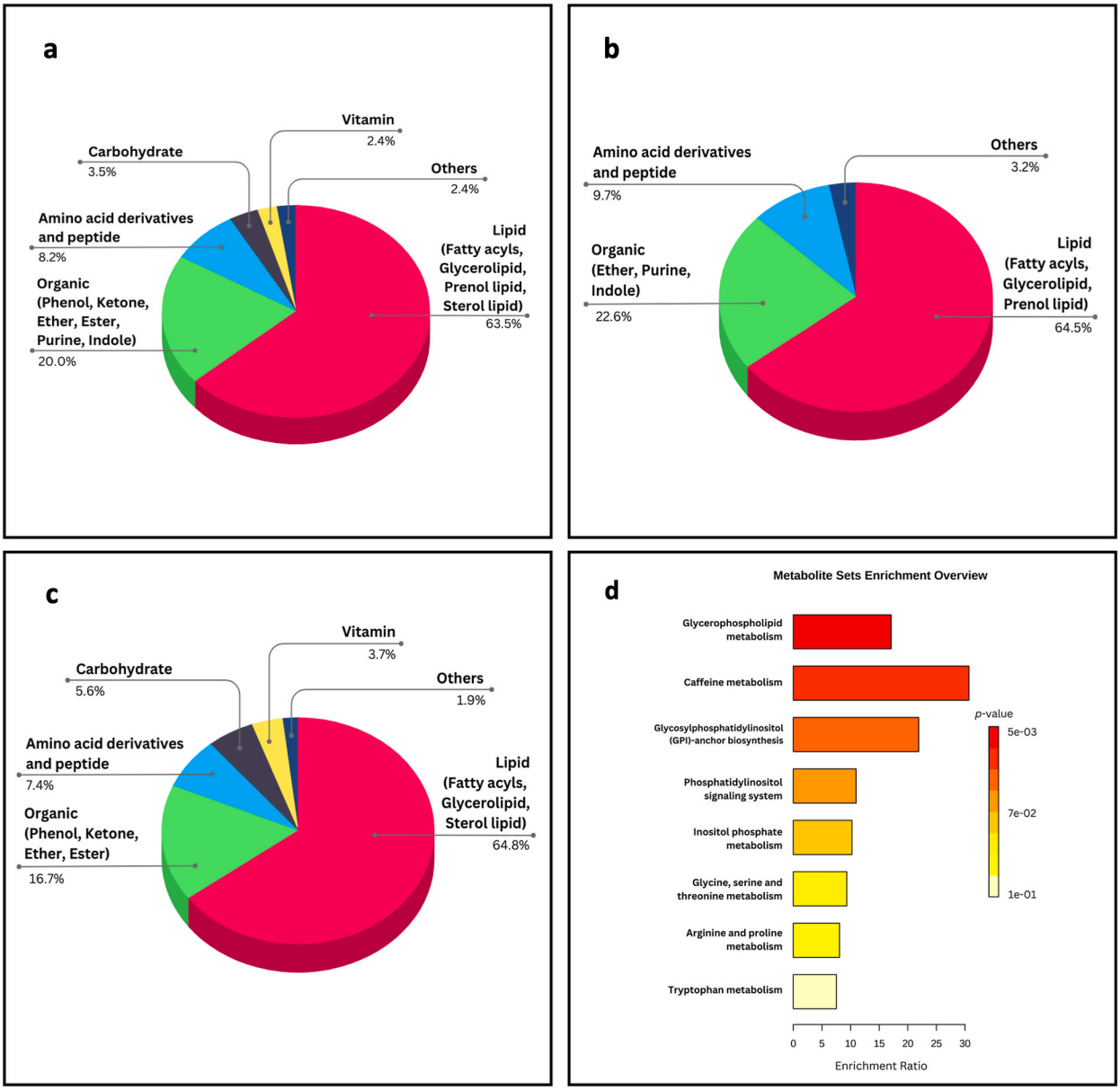

Fig. 4. Classification was conducted for (a) all significant metabolites, (b) significantly upregulated metabolites, and (c) significantly down-regulated metabolites observed in obese individuals. Lipids emerged as the predominant category among the altered metabolites in obesity. (d) Over-representation analysis underscores glycerophospholipid metabolism as the most significantly affected pathway in our dataset.

4. Discussion

The normal weight Body Mass Index (BMI) range is typically 18.5–24.9 kg/m^2, and obesity is classified as a BMI of ≥30 kg/m^2. This study uses a narrower normal BMI range of 18.5–22.9 kg/m^2, while maintaining the obesity threshold at ≥ 30 kg/m^2. The adjustment was made because individuals of Asian descent tend to have a higher proportion of body fat at a given BMI compared to Caucasians, leading to a greater risk of obesity-related health issues even at lower BMI levels [22]. Overweight participants were excluded from this study, creating a wide gap of 6.9 kg/m^2 between the BMI ranges of 23–29.9 kg/m^2 for cases and controls. To reinforce our selection criteria, only participants whose BMI classification remained stable across two consecutive appointments were included. Maintaining a consistent BMI across two time points helps minimize variations in the pattern and magnitude of any metabolic changes [23]. Additionally, the body composition data of the chosen participants revealed highly significant differences between the case and control groups. This approach helped ensure the study was designed to reflect extreme conditions in both groups.

Metabolites possess dynamic characteristics that provide insights into an individual's metabolic state. Comparing metabolomics

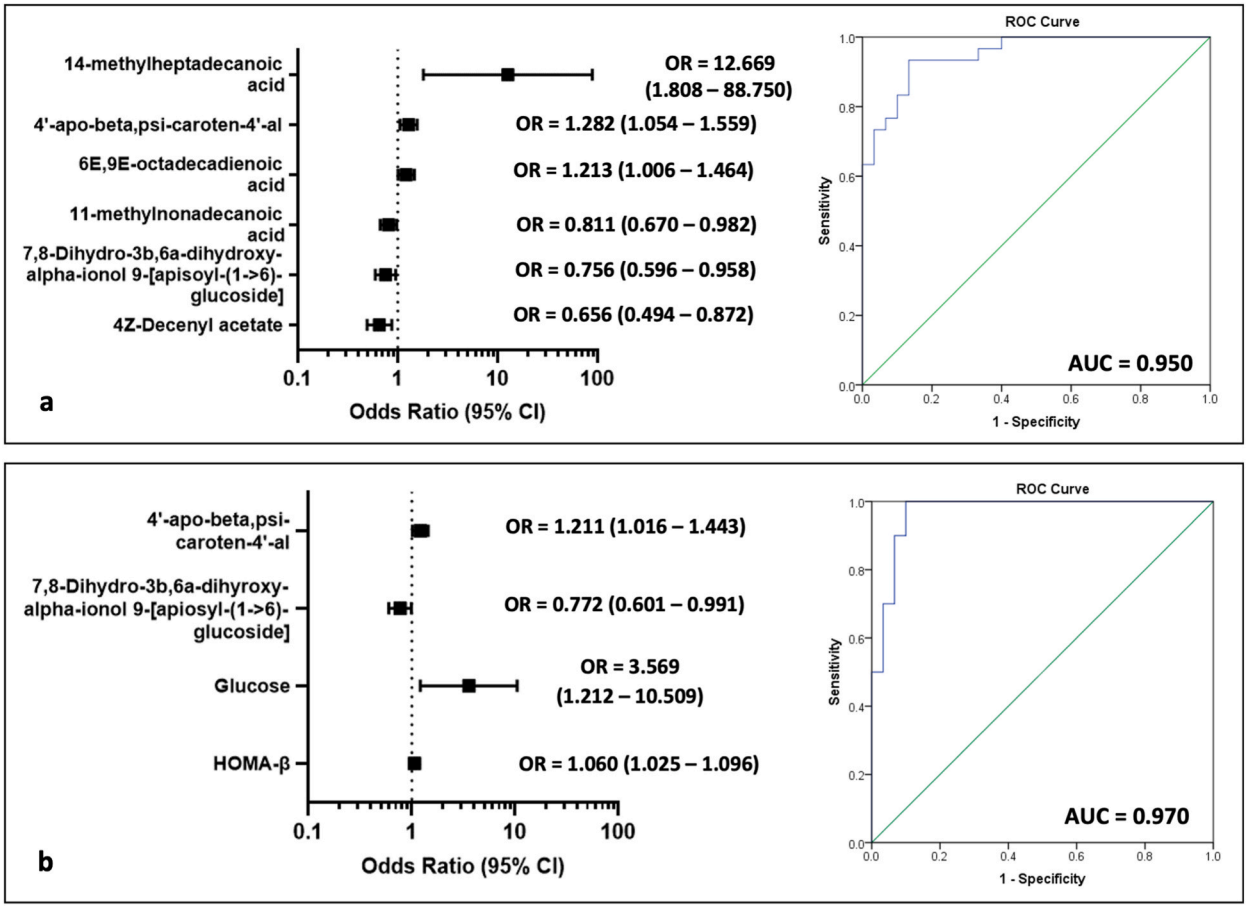

Fig. 5. Prediction model for (a) metabolites, and (b) the combination of metabolites and clinical parameters associated with obesity risk. All models were developed using stepwise multiple logistic regression and ROC curve analysis.

data across different cohorts is challenging, as metabolite levels are easily influenced by participants' lifestyle factors such as circadian rhythms, dietary intake, sleep patterns, and physical activity. Additionally, natural metabolic flux, and single, snapshot, moment-in-time measurements contribute to variability in findings. Despite these challenges, the rising prevalence of obesity in Malaysia underscores the necessity of delving into the field of metabolomics. Consequently, this investigation unveiled a discernible disparity of the metabolite profiles between lean and obese individuals, as evidenced by the PLS-DA plot.

Our predictive model revealed that 4′-apo-beta,psi-caroten-4′-al, elevated fasting blood glucose and HOMA-β are associated with the increased risk of obesity while 7,8-Dihydro-3b,6a-dihydroxy-alpha-ionol 9-[apiosyl-(1->6)-glucoside] are indicators of reduced risk of obesity in the study population. Interestingly, 4′-apo-beta,psi-caroten-4′-al is a lipid metabolite that demonstrates the most notable difference in expression levels between obese and lean individuals. Elevated lipid levels are consistently associated with excess body fat in obese individuals [24,25]. Our findings corroborate this association, revealing that lipid class is the most prominently detected entity. Furthermore, the sub-pathway of lipid metabolism, specifically glycerophospholipid metabolism, emerges as the most significantly altered in obesity. The pattern of disturbance in the pathway is also reported in patients with coronary artery disease [26] and type 2 diabetes mellitus [27]. The lack of rigidity in plasma membranes can lead to alteration in receptor accessibility. Consequently, the remodelling of this pathway, mediated by lysophosphatidylcholine acyltransferase (LPCAT3), has been shown to suppress insulin sensitivity and affects glucose uptake in obese individuals [28]. Additionally, caffeine metabolism emerged as the most enriched pathway, prompting questions about whether the presence of circulating metabolites is a result of excessive caffeine consumption or genuinely influenced by obesity. Although an increased dietary intake of caffeine has been associated with reduced body fat [29], it is worth noting that excessive caffeine intake may raise cortisol levels which can promote overeating, potentially accounting for the variations in our research findings [30,31].

The metabolomic techniques employed in this study have not only enabled the identification of metabolites associated with disease prognosis and risk but also provided a basis for developing prevention and intervention strategies tailored to individual profiles. For instance, our investigation identified 14-methylheptadecanoic acid, 4′-apo-beta,psi-caroten-4′-al, and 6E,9E-octadecadienoic acid as metabolites associated with higher obesity risk, while 19:0 (11Me), 7,8-Dihydro-3b,6a-dihydroxy-alpha-ionol 9-[apiosyl-(1->6)-glucoside], and 4Z-Decenyl acetate were linked to reduced risk. These findings underscore the potential of metabolomic data to inform

Table 2
Comparison of the same prediction model using different machine learning algorithms.

Machine Learning Algorithm	Predictive Accuracy	Receiving Operating Characteristics (ROC)	Prediction Class Probability
PLS-DA	0.735	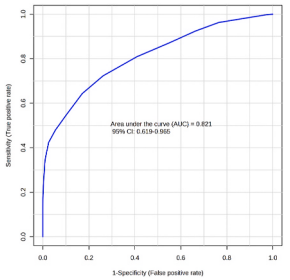	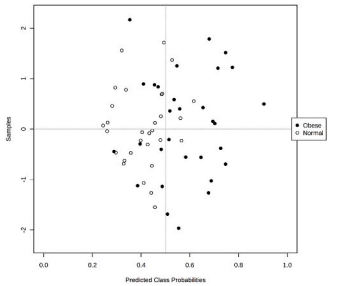
Random Forest	0.797	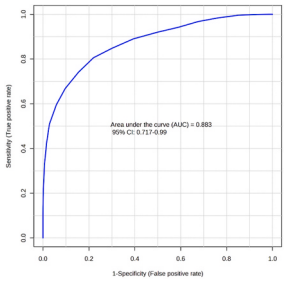	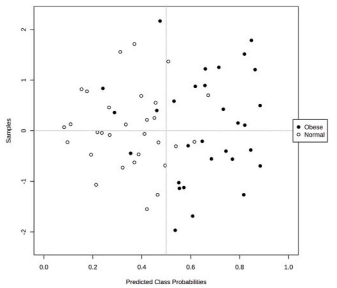
Linear SVM	0.802	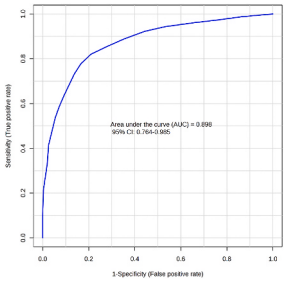	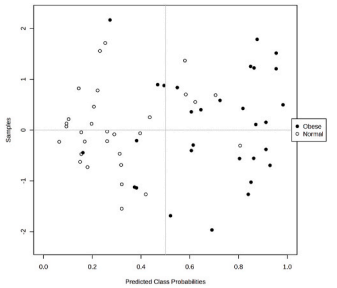
Logistic Regression	0.821	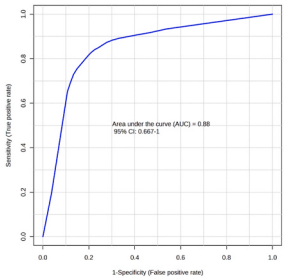	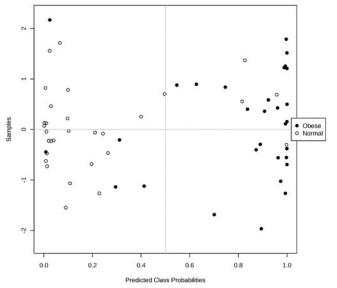

Table 3
Key metabolites and their attributes in the obesity prediction model.

Metabolite	Metabolite ID (HMDB/PubChem)	Class	Study power (%)	Effect size
14-methylheptadecanoic acid	HMDB0340353	Lipid	100	0.77
4′-apo-beta,psi-caroten-4′-al	44224033	Prenol Lipid	100	0.58
6E,9E-octadecadienoic acid	5312481	Lipid	100	0.50
19:0(11Me)	HMDB0340386	Lipid	98.1	0.73
7,8-Dihydro-3b,6a-dihydroxy-alpha-ionol 9-[apiosyl-(1->6)-glucoside]	HMDB0041579	Carbohydrate	86.8	0.52
4Z-Decenyl acetate	HMDB0032214	Lipid	61.0	0.63

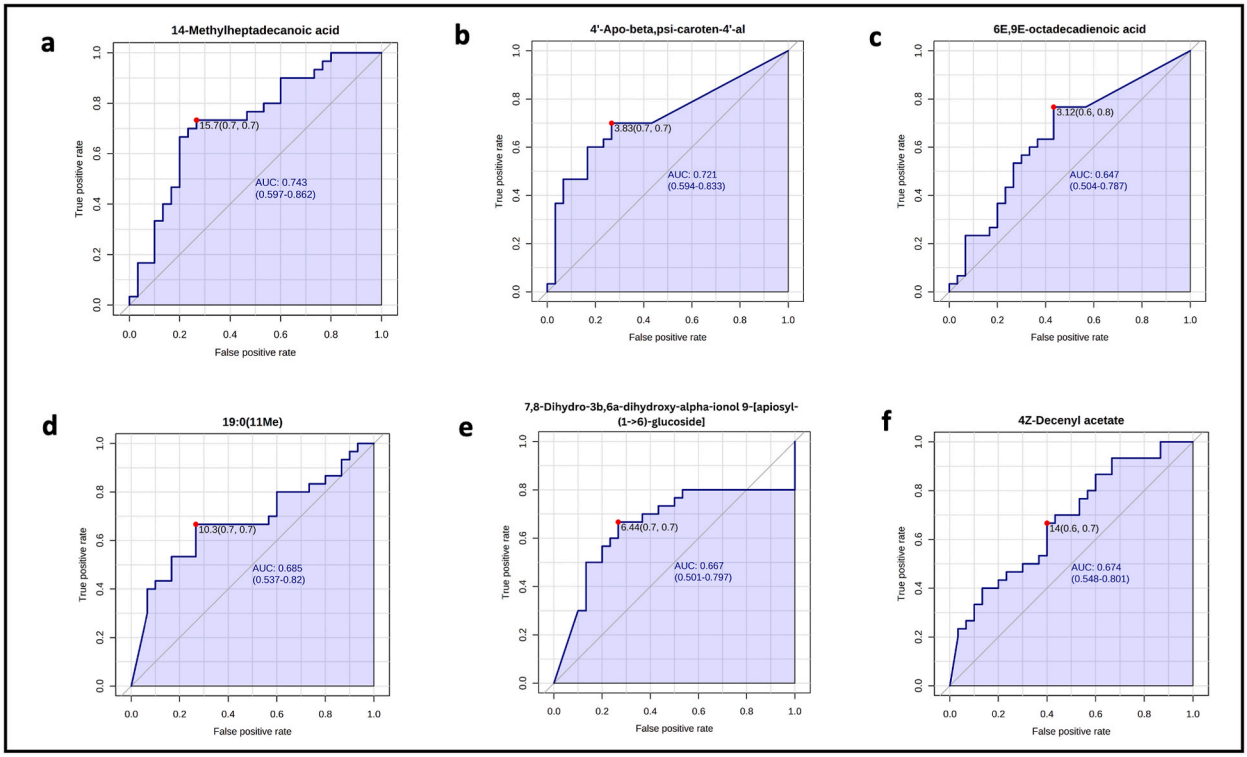

Fig. 6. ROC curve of individual metabolites involved in the prediction model. High-risk metabolites include (a) 14-methylheptadecanoic acid, (b) 4′-apo-beta,psi-caroten-4′-al and (c) 6E,9E-octadecadienoic acid. Low-risk metabolites comprise (d) 19:0(11Me), (e) 7,8-Dihydro-3b,6a-dihydroxy-alpha-ionol 9-[apiosyl-(1->6)-glucoside] and (f) 4Z-Decenyl acetate.

personalized approaches to obesity prevention.

Previous studies have reported that both β-carotene and vitamin A levels are reduced in obese individuals [32,33]. Additionally, some studies suggest that vitamin A supplementation may contribute to reducing body fat [34], and its deficiency has been linked to obesity [35]. However, the precise role of vitamin A in regulating adipose tissue remains unclear. Given that β-carotene, the most abundant carotenoid, serves as a precursor to vitamin A, we are particularly interested in investigating the role of β-carotene in obesity. Its potential therapeutic and preventive effects are promising areas of ongoing research.

A notable instance is the metabolite 4′-apo-beta,psi-caroten-4′-al, derived from the oxidative degradation of β-carotene, which has been shown in this study to be elevated in individuals with obesity. This elevation suggests a possible disruption in the conversion of β-carotene to vitamin A, a process integral to maintaining metabolic health. Previous studies have linked vitamin A deficiency to obesity and highlighted the regulatory effects of β-apocarotenals on key metabolic pathways, such as the repression of peroxisome proliferator-activated receptor (PPAR) signaling and retinoid X receptor (RXR) activation during adipocyte differentiation [36]. The inhibition of the PPAR/RXR heterodimer interferes with insulin signaling, leading to reduced glucose uptake and elevated glucose levels in circulation (Fig. 8) [37].

In this study, the findings that 4′-apo-beta,psi-caroten-4′-al, glucose, and HOMA-β are associated with an increased risk of obesity provide valuable insights for developing personalized prevention strategies. Targeting these metabolites could pave the way for interventions aimed at restoring disrupted metabolic pathways and mitigating obesity risk at an individual level. These findings highlight the dual utility of metabolomic research: advancing biomarker identification while fostering a deeper understanding of individualized disease mechanisms and prevention strategies.

Additionally, branched-chain fatty acids (BCFAs), a subset of saturated fatty acids distinguished by the inclusion of a methyl group within their chemical structure, were examined in our study. Among these, two significant metabolites were identified: 14-methylheptadecanoic acid and 19:0(11Me). Interestingly, these metabolites appeared to be reduced in obese individuals, despite the typical abundance of fatty acids in obesity [38]. Our data revealed contrasting trends for these two metabolites, potentially attributable to differences in their molecular conformations [39]. Structural variations in lipids may influence the activities of key lipogenic enzymes [40], offering a plausible explanation for the divergent findings observed. However, the exact mechanisms underlying their function remain unclear, though they are suggested to be linked to oxidation processes involved in catabolism. This nuanced understanding underscores the complexity of metabolic pathways and highlights the importance of continued research to elucidate these mechanisms.

Another metabolite, 6E,9E-octadecadienoic acid, an unsaturated fatty acid derived from linoleic acid, was also examined. Elevated levels of this metabolite suggest a potential disruption in the conversion to arachidonic acid, a substrate for the production of

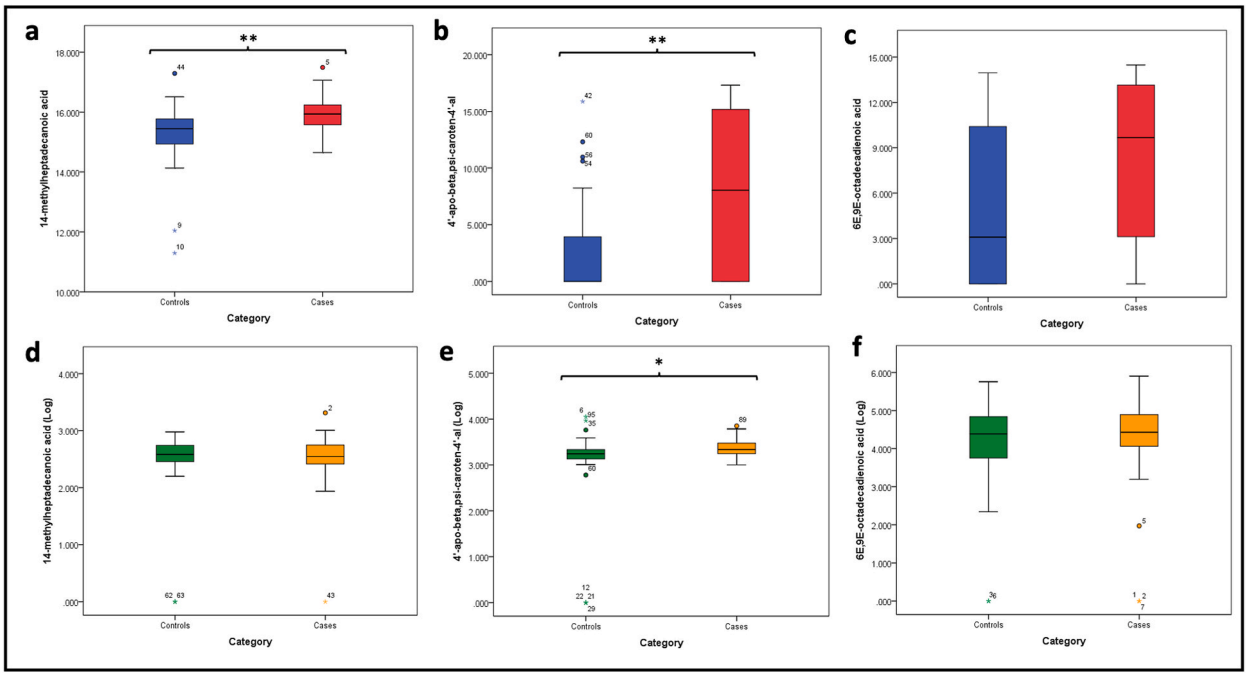

Fig. 7. Box-plot abundance of high-risk metabolites in discovery and validation phases. Differential analysis for discovery phase includes independent *t*-test for (a) 14-methylheptadecanoic acid, (b) 4′-apo-beta,psi-caroten-4′-al and (c) 6E,9E-octadecadienoic acid. Similarly, for validation phase, (d) 14-methylheptadecanoic acid, (e) 4′-apo-beta,psi-caroten-4′-al and (f) 6E,9E-octadecadienoic acid. ** indicates *p*-value <0.01, and * indicates *p*-value <0.05.

eicosanoids. Eicosanoids function as signalling molecules in the regulation of inflammatory and immune responses [41,42]. These findings shed light on the intricate metabolic pathways associated with obesity and underscore the importance of further research to elucidate the underlying mechanisms.

Higher levels of the three high-risk metabolites, 14-methylheptadecanoic acid, 4′-apo-beta,psi-caroten-4′-al, and 6E,9E-octadecadienoic acid, may be similarly connected to obesity. Fig. 8 illustrates the potential mechanisms through which these metabolites could contribute to obesity. These metabolites are suggested to be involved in the activation of the PPAR/RXR heterodimer, which influences adipokine transcription, regulates inflammation, and contributes to lipid metabolism.

To date, only a handful of studies have identified the remaining two metabolites associated with lower risk: 7,8-Dihydro-3b,6a-dihydroxy-alpha-ionol 9-[apiosyl-(1->6)-glucoside] and 4Z-Decenyl acetate. Our understanding of the interplay between these mechanisms in the context of obesity remains limited. According to the HMDB and PubChem database, these two metabolites were classified as a carbohydrate and a lipid, respectively. The decrease in these metabolites suggests a potential disruption in energy production and an excessive storage pattern in obese individuals. Therefore, further investigations into these two entities are imperative to gain deeper insights into their association with obesity and its metabolic implications.

In the present study, among the three high-risk metabolites, our data consistently showed 4′-apo-beta,psi-caroten-4′-al to be significantly upregulated in cases compared to controls, across both discovery and validation datasets. Despite the disparity observed in other metabolites, the patterns in both phases are identical. The diluted results may stem from differences in participant characteristics criteria; notably, the mean BMI values between cases and controls were significantly closer in both groups in the validation phase compared to the discovery phase. It is recognized that metabolite levels are dynamic and sampling variability could influence their concentrations [43]. Moreover, the MS2 ion scan resolution for metabolite identification exhibits greater sensitivity than MS1, attributed to the precision of metabolite fragmentation [44]. Consequently, we employed both MS1 and MS2 approaches in this study aimed at enhancing the dynamic range and improving metabolite reproducibility.

Although the sample size in the discovery phase appears small, we believe it does not significantly affect the quality of this study. The statistical power of the shortlisted metabolites in the model exceeds 80 % for most, with the exception of 4Z-Decenyl acetate. Thus, despite starting with 30 samples per group, we consider our data to be sufficient for providing valuable and reliable insights. Subsequently, the required sample size for the validation phase was determined based on calculations from the discovery phase, with a maximum of 46 samples.

Obesity affects individuals of all ages, from childhood to older adulthood. In this study, some participants were over 70 years old, potentially experiencing sarcopenic obesity, a condition that was not assessed. Moreover, lifestyle factors such as diet includes the caffeinated beverages intake, physical activity, and sleep quality are potential contributors to obesity. However, this valuable data is not available to account for the confounding factors in the analysis.

Another limitation of this research lies in the incapacity of mass spectrometry to distinguish between isomers. Consequently,

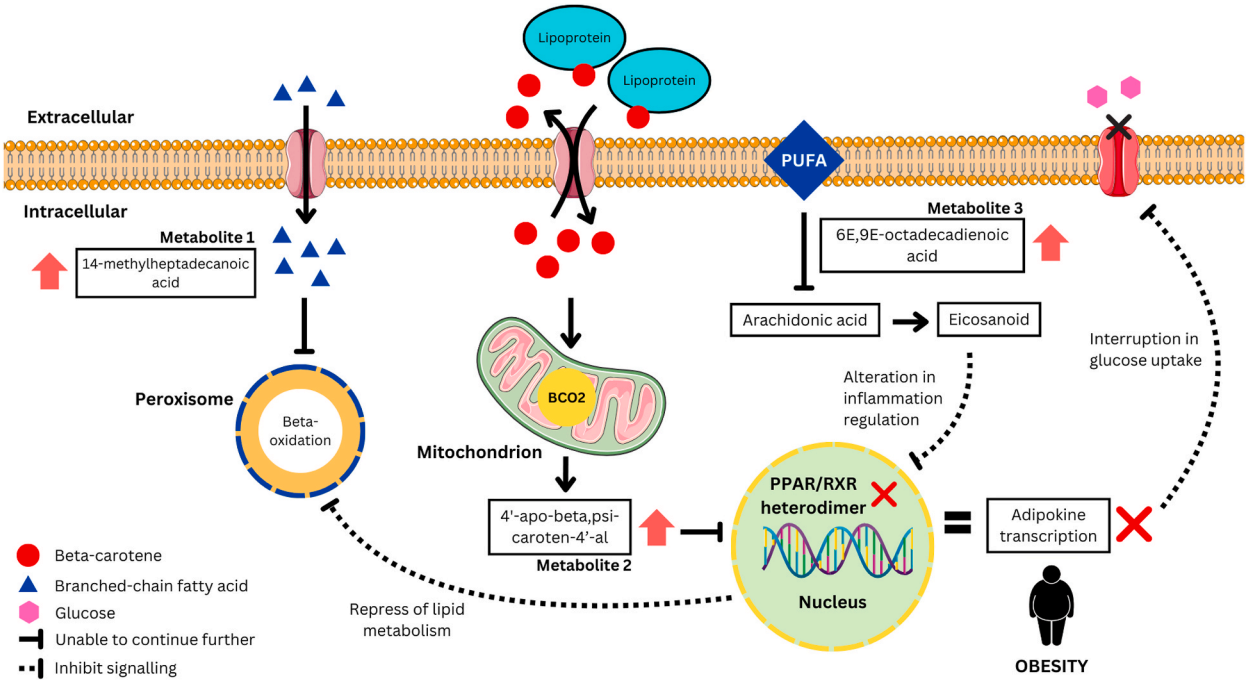

Fig. 8. A snapshot of suggested mechanisms for three metabolites associated with increased risk of obesity. Higher level of 14-methylheptadecanoic acid (Metabolite 1) appears to be incapable of further oxidation for energy generation. Next, the elevated presence of 4′-apo-beta,psi-caroten-4'al (Metabolite 2) in obesity is suggested to suppress the formation of PPAR/RXR heterodimers and halt the transcription of adiponectin. This causes the interruption in glucose uptake and contributes to hyperglycaemia in obese individuals. On top of that, an increase level of 6E,9E-octadecadienoic acid (Metabolite 3) signify a disruption in the production of eicosanoids, which serve as agonist to activate PPAR/RXR. The deactivation of the PPAR/RXR complex appears to be the most likely link between these metabolites in their contribution to the development of obesity. It is recognized that PPAR plays a role in lipid and glucose metabolism, as well as in the regulation of inflammation.

quantifying these potential metabolites can offer a clearer understanding of the variations in metabolite levels between obese and lean individuals. Although the comparison relies on relative abundance, this study provides a distinctive advantage by encompassing participants from diverse ethnicities and cultural backgrounds within a single investigation. Furthermore, the strategic use of MS1 during the discovery phase and MS2 in the validation phase aims to mutually enhance metabolite identification efforts [45].

5. Conclusions

Untargeted metabolomics analysis plays a crucial role in identifying novel biomarkers essential for comprehending the intricate mechanisms underlying obesity. The identification of three metabolites linked to high-risk (14-methylheptadecanoic acid, 4′-apo-beta, psi-caroten-4'al and 6E,9E-octadecadienoic acid) suggests potential disruptions in lipid and glucose metabolism among obese individuals in a selected Malaysian population. These findings represent a significant stride in bridging the knowledge gap and advancing our scientific comprehension of this multifaceted condition. Furthermore, they underscore the prominence of lipids in obesity-related metabolic alterations and highlight their potential as biomarkers for metabolic dysregulation associated with obesity.

CRediT authorship contribution statement

Anis Adibah Osman: Writing – review & editing, Writing – original draft, Investigation, Formal analysis. **Siok-Fong Chin:** Writing – review & editing, Writing – original draft, Visualization, Supervision, Methodology, Conceptualization. **Lay-Kek Teh:** Writing – review & editing. **Noraidatulakma Abdullah:** Writing – review & editing, Methodology, Conceptualization. **Nor Azian Abdul Murad:** Writing – review & editing. **Rahman Jamal:** Writing – review & editing, Supervision, Methodology, Funding acquisition, Conceptualization.

Ethics statement

Ethics approval for this project was obtained from the Research Ethics Committee of Universiti Kebangsaan Malaysia (REC UKM), with reference number JEP-2021-344.

Declaration of competing interest

The authors declare that there is no conflict of interest exists.

Acknowledgement

The authors extend their gratitude to the Ministry of Health, Malaysia for providing study leave during the research process. Additionally, special appreciation is owed to NEWTON-MRC/2020/004 and Ministry of Higher Education, Malaysia - The Malaysian Cohort under PDE 48 grant for their financial support. The authors would also like to acknowledge the assistance of the staff of The Malaysian Cohort, particularly Ms. Nazihah Jalal and Ms. Azwa Shawani Kamalul Arifin, for their help with sample and data retrieval. Furthermore, thanks are due to the iPROMISE's director and research fellow, Prof. Dr. Mohd Zaki Salleh and Dr. Mohd Salleh Rofiee, for granting permission to use instrumentation and technical guidance.

Appendix A. Supplementary data

Supplementary data to this article can be found online at https://doi.org/10.1016/j.heliyon.2025.e42197.

References

[1] WHO, Obesity: Preventing and Managing the Global Epidemic, World Health Organization, 2000.
[2] Institute for Public Health (IPH), N.I.o.H., Ministry of Health Malaysia, National Health and Morbidity Survey (NHMS) 2019, NCDs – Non-communicable Diseases: Risk Factors and Other Health Problems, vol. I, 2019.
[3] J.P. Hamilton, Epigenetics: principles and practice, Dig. Dis. 29 (2) (2011) 130–135.
[4] R.J.F. Loos, G.S.H. Yeo, The genetics of obesity: from discovery to biology, Nat. Rev. Genet. 23 (2) (2022) 120–133.
[5] K. Rohde, et al., Genetics and epigenetics in obesity, Metabolism 92 (2019) 37–50.
[6] C. Guijas, et al., Metabolomics activity screening for identifying metabolites that modulate phenotype, Nat. Biotechnol. 36 (4) (2018) 316–320.
[7] M.J. Sohn, et al., Metabolomic signatures for the effects of weight loss interventions on severe obesity in children and adolescents, Metabolites 12 (1) (2021).
[8] R.G. Duft, et al., Altered metabolomic profiling of overweight and obese adolescents after combined training is associated with reduced insulin resistance, Sci. Rep. 10 (1) (2020) 16880.
[9] A.M. Brennan, et al., Plasma metabolite profiles in response to chronic exercise, Med. Sci. Sports Exerc. 50 (7) (2018) 1480–1486.
[10] H. Hanamatsu, et al., Altered levels of serum sphingomyelin and ceramide containing distinct acyl chains in young obese adults, Nutr. Diabetes 4 (2014) e141.
[11] C.A. Pickens, et al., Plasma phospholipids, non-esterified plasma polyunsaturated fatty acids and oxylipids are associated with BMI, Prostaglandins Leukot. Essent. Fatty Acids 95 (2015) 31–40.
[12] M. Bagheri, et al., Obesity-related metabolomic profiles and discrimination of metabolically unhealthy obesity, J. Proteome Res. 17 (4) (2018) 1452–1462.
[13] V.H. Telle-Hansen, et al., A comprehensive metabolic profiling of the metabolically healthy obesity phenotype, Lipids Health Dis. 19 (1) (2020) 90.
[14] F. Vanweert, P. Schrauwen, E. Phielix, Role of branched-chain amino acid metabolism in the pathogenesis of obesity and type 2 diabetes-related metabolic disturbances BCAA metabolism in type 2 diabetes, Nutr. Diabetes 12 (1) (2022) 35.
[15] P. Bellot, et al., Plasma lipid metabolites as potential biomarkers for identifying individuals at risk of obesity-induced metabolic complications, Sci. Rep. 13 (1) (2023) 11729.
[16] D. Albuquerque, et al., The contribution of genetics and environment to obesity, Br. Med. Bull. 123 (1) (2017) 159–173.
[17] R. Jamal, et al., Cohort Profile: the Malaysian Cohort (TMC) project: a prospective study of non-communicable diseases in a multi-ethnic population, Int. J. Epidemiol. 44 (2) (2015) 423–431.
[18] C. Schiffman, et al., Filtering procedures for untargeted LC-MS metabolomics data, BMC Bioinf. 20 (1) (2019) 334.
[19] L.A. Dahabiyeh, et al., Diagnosing Parkinson's disease and monitoring its progression: biomarkers from combined GC-TOF MS and LC-MS/MS untargeted metabolomics, Heliyon 10 (9) (2024) e30452.
[20] F. Wang, et al., CFM-ID 4.0: more accurate ESI-MS/MS spectral prediction and compound identification, Anal. Chem. 93 (34) (2021) 11692–11700.
[21] G.M. Sullivan, R. Feinn, Using effect size-or why the P value is not enough, J. Grad. Med. Educ. 4 (3) (2012) 279–282.
[22] WHO, Appropriate body-mass index for Asian populations and its implications for policy and intervention strategies, Lancet 363 (9403) (2004) 157–163.
[23] D.M. Lloyd-Jones, et al., Consistently stable or decreased body mass index in young adulthood and longitudinal changes in metabolic syndrome components: the Coronary Artery Risk Development in Young Adults Study, Circulation 115 (8) (2007) 1004–1011.
[24] S.U. Shahid Shabana, S. Sarwar, The abnormal lipid profile in obesity and coronary heart disease (CHD) in Pakistani subjects, Lipids Health Dis. 19 (1) (2020) 73.
[25] H. Kiriyama, et al., Association between changes in body weight and lipid profile in the general population: a community-based cohort study, Eur. Heart J. Qual. Care Clin. Outcomes 7 (1) (2021) 109–110.
[26] H. Chen, et al., Comprehensive metabolomics identified the prominent role of glycerophospholipid metabolism in coronary artery disease progression, Front. Mol. Biosci. 8 (2021) 632950.
[27] S. Chen, et al., Associations of plasma glycerophospholipid profile with modifiable lifestyles and incident diabetes in middle-aged and older Chinese, Diabetologia 65 (2) (2022) 315–328.
[28] P.J. Ferrara, et al., Lysophospholipid acylation modulates plasma membrane lipid organization and insulin sensitivity in skeletal muscle, J. Clin. Invest. 131 (8) (2021).
[29] A. Lee, et al., Coffee intake and obesity: a meta-analysis, Nutrients 11 (6) (2019).
[30] A. Haraguchi, et al., Caffeine suppresses high-fat diet-induced body weight gain in mice depending on feeding timing, J. Funct.Foods 99 (2022) 105307.
[31] W.R. Lovallo, et al., Cortisol responses to mental stress, exercise, and meals following caffeine intake in men and women, Pharmacol. Biochem. Behav. 83 (3) (2006) 441–447.
[32] C. Wang, et al., Associations of serum carotenoids with DXA-derived body fat and fat distribution in Chinese adults: a prospective study, J. Acad. Nutr. Diet. 120 (6) (2020) 985–1001.
[33] G. Marcelino, et al., Beta-carotene: preventive role for type 2 diabetes mellitus and obesity: a review, Molecules 25 (24) (2020).
[34] S.M. Jeyakumar, A. Vajreswari, N.V. Giridharan, Chronic dietary vitamin A supplementation regulates obesity in an obese mutant WNIN/Ob rat model, Obesity 14 (1) (2006) 52–59.
[35] N. Yao, et al., The association between carotenoids and subjects with overweight or obesity: a systematic review and meta-analysis, Food Funct. 12 (11) (2021) 4768–4782.

[36] O. Ziouzenkova, et al., Asymmetric cleavage of beta-carotene yields a transcriptional repressor of retinoid X receptor and peroxisome proliferator-activated receptor responses, Mol. Endocrinol. 21 (1) (2007) 77–88.
[37] S. Sharma, et al., Retinoid X receptor: cellular and biochemical roles of nuclear receptor with a focus on neuropathological involvement, Mol. Neurobiol. 59 (4) (2022) 2027–2050.
[38] A. Pakiet, et al., The effect of one anastomosis gastric bypass on branched-chain fatty acid and branched-chain amino acid metabolism in subjects with morbid obesity, Obes. Surg. 30 (1) (2020) 304–312.
[39] P. Gozdzik, et al., Branched-chain fatty acids affect the expression of fatty acid synthase and C-reactive protein genes in the hepatocyte cell line, Biosci. Rep. 43 (10) (2023).
[40] A. Czumaj, T. Sledzinski, A. Mika, Branched-chain fatty acids alter the expression of genes responsible for lipid synthesis and inflammation in human adipose cells, Nutrients 14 (11) (2022).
[41] F. Haghighatdoost, M.G.B.F. Nobakht, Effect of conjugated linoleic acid on blood inflammatory markers: a systematic review and meta-analysis on randomized controlled trials, Eur. J. Clin. Nutr. 72 (8) (2018) 1071–1082.
[42] W. Wang, et al., Effects of high-fat diet on plasma profiles of eicosanoid metabolites in mice, Prostag. Other Lipid Mediat. 127 (2016) 9–13.
[43] C. Beuchel, et al., Clinical and lifestyle related factors influencing whole blood metabolite levels - a comparative analysis of three large cohorts, Mol. Metabol. 29 (2019) 76–85.
[44] T. Huang, et al., Combining precursor and fragment information for improved detection of differential abundance in data independent acquisition, Mol. Cell. Proteomics 19 (2) (2020) 421–430.
[45] J.F. Xiao, B. Zhou, H.W. Ressom, Metabolite identification and quantitation in LC-MS/MS-based metabolomics, Trends Anal. Chem. 32 (2012) 1–14.